Intelligent Reflecting Surfaces for Enhanced Physical Layer Security in NOMA VLC Systems

Hanaa Abumarshoud, Cheng Chen, Iman Tavakkolnia, Harald Haas, and Muhammad Ali Imran.

Abstract—The rise of intelligent reflecting surfaces (IRSs) is opening the door for unprecedented capabilities in visible light communication (VLC) systems. By controlling light propagation in indoor environments, it is possible to manipulate the channel conditions to achieve specific key performance indicators. In this paper, we investigate the role that IRSs can play in boosting the secrecy capacity of non-orthogonal multiple access (NOMA) VLC systems. More specifically, we propose an IRS-based physical layer security (PLS) mechanism that mitigates the information leakage risk inherent in NOMA. Our results demonstrate that the achieved secrecy capacity can be enhanced by up to 105% for a number of 80 IRS elements. To the best of our knowledge, this is the first paper that examines the PLS of NOMA-based IRS-assisted VLC systems.

Index Terms—visible light communication (VLC), light fidelity (LiFi), intelligent reflecting surface (IRS), non-orthogonal multiple access (NOMA), physical layer security (PLS).

I. INTRODUCTION

Visible light communication (VLC) has gained significant interest in the last decade, which has been manifested by extensive research studies as well as practical implementations from academia and industry alike. Based on VLC, the concept of light fidelity (LiFi) started to take shape as a fully networked solution for bi-directional high-speed connectivity with multiple access support [1, 2]. Different optical multiple access schemes have been investigated in order to facilitate ubiquitous multi-user connectivity in LiFi. Multiple access can be broadly divided into two categories: orthogonal multiple access (OMA) and non-orthogonal multiple access (NOMA). OMA allocates orthogonal resources to the users either in the frequency domain, by means of orthogonal frequency division multiple access (OFDMA), or the time domain, by means of time division multiple access (TDMA). NOMA schemes enable multiple users of accessing the same bandwidth and time resources by allocating distinct power levels, in the case of power-domain NOMA, or distinct codes, in the case of code division multiple access (CDMA) [3, 4]. In this paper, we refer to power-domain NOMA as NOMA.

NOMA is considered a promising solution for boosting the spectral efficiency of VLC, mainly due to the inherent high signal-to-noise-ratio (SNR) in indoor VLC systems. To implement NOMA, superposition coding is performed at the access point (AP). In this step, distinct power levels are assigned to the different users' signals. The power allocation coefficients are typically decided based on the relative users' channel conditions such that users with higher channel gains are assigned lower power levels, and vice versa. At the receiver side, successive interference cancellation (SIC) is performed to decode and subtract the signals with higher power levels first until the desired signal is extracted. SIC implies that users with higher decoding order, i.e., users allocated less power, can successfully decode the signals of the users with lower decoding order. This presents a security gap in NOMA-based communications if one of the network users is malicious.

The concept of intelligent reflecting surfaces (IRSs) has recently evolved as a focal point of interest in the wireless communication community as it offers a spectrum, energy, and cost-efficient approach for sustainable evolution in wireless systems. An IRS constitutes a number of reflecting elements (REs) that can be artificially engineered in order to control their response to incident light rays. Based on this, it is possible to effectively control the propagation of the light signals to achieve desired performance gains. A detailed overview of the advantages and challenges related to the integration of IRS technology in the context of VLC and LiFi systems is presented in [5]. Recent research efforts have considered VLC performance evaluation and enhancement in IRS-enabled environments. For example, the energy efficiency maximisation of IRS-assisted VLC systems was investigated in [6] while [7] considered the optimisation of the IRS reflection coefficients with the objective of sum-rate maximisation. In [8], a framework for an IRS-assisted NOMA VLC system was presented with the objective of enhancing the link reliability.

In this paper, we propose a physical layer security (PLS) mechanism for IRS-assisted NOMA VLC systems. The term PLS refers to the techniques that exploit the physical properties of the optical channel to secure the transmission of information against potential eavesdroppers [9, 10, 11]. Assuming that network users are assigned a trust score, i.e., based on their previous activity, we formulate a problem to maximise the secrecy capacity of a trusted user while maintaining minimum rate constraints for the untrusted user. This is achieved by jointly optimising the NOMA power allocation and the IRS configuration based on the given system parameters, users' locations, and rate requirements. We propose a novel PLS strategy and an alternating optimisation algorithm that utilises the adaptive-restart genetic algorithm (GA) in order to obtain a computationally efficient solution. The rest of the paper is organised as follows: the system model and problem statement are presented in Section II. The proposed joint IRS configuration and power allocation scheme is discussed in Section III.

Hanaa Abumarshoud and Muhammad Ali Imran are with James Watt School of Engineering, University of Glasgow, Glasgow, UK (e-mail:{hanaa.abumarshoud, Muhammad.Imran}@glasgow.ac.uk).

Cheng Chen, Iman Tavakkolnia, and Harald Haas are with the LiFi R&D Centre, University of Strathclyde, Glasgow, UK (e-mail:{c.chen,i.tavakkolnia, harald.haas}@strath.ac.uk).

Simulation results are shown in Section IV and the paper is concluded in Section V.

II. SYSTEM MODEL

We consider a NOMA-based VLC network consisting of one AP, two paired users, and N REs, as depicted in Fig. 1. It is noted that typical systems employing NOMA divide users into multiple orthogonal pairs, i.e., in the time or frequency domain, and NOMA is implemented within each pair. As such, the users in this scenario may correspond to a NOMA pair in a hybrid NOMA/OMA network. Without loss of generality, we assume that the user locations and VLC channel state information (CSI) are available at a central control unit where the resource allocation decisions are made.
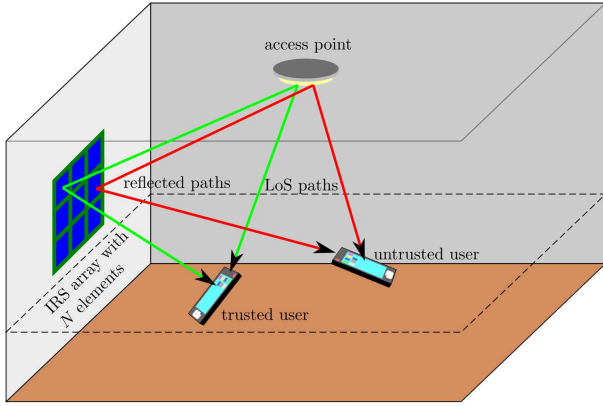

Fig. 1: System model with two NOMA users: trusted and untrusted. The goal is to secure the transmission of the trusted user while satisfying given rate constraints.

A. Channel gain of LoS paths

The line-of-sight (LoS) channel gain from the light-emitting diode (LED) to the k-th user's photo-detector (PD) is given by

$$h_{k,\text{LED}}^{\text{LoS}} = \mathcal{V}_{k,\text{LED}}^{\text{LoS}} \cos^m(\phi_{k,\text{LED}}) \cos(\psi_{k,\text{LED}}), \quad (1)$$

for $0 \leq \psi_{k,\text{LED}} \leq \Psi_c$ and 0 otherwise, where

$$\mathcal{V}_{k,\text{LED}}^{\text{LoS}} = \frac{A(m+1)}{2\pi d_{k,\text{LED}}^2} \mathcal{G}_f \mathcal{G}_c, \quad (2)$$

where $d_{k,\text{LED}}$ denotes the Euclidean distance from the LED to the k-th user; A is the physical area of the PD; $\phi_{k,\text{LED}}$ is the angle of irradiance with respect to the axis normal to the LED plane; $\psi_{k,\text{LED}}$ is the angle of incidence with respect to the axis normal to the receiver plane. From analytical geometry, the irradiance and incidence angles can be calculated as

$$\cos(\phi_{k,\text{LED}}) = \frac{\mathbf{d}_{k,\text{LED}} \cdot \mathbf{n}_{\text{LED}}}{\|\mathbf{d}_{k,\text{LED}}\|}, \quad (3a)$$

$$\cos(\psi_{k,\text{LED}}) = \frac{-\mathbf{d}_{k,\text{LED}} \cdot \mathbf{n}_{\text{PD}}}{\|\mathbf{d}_{k,\text{LED}}\|}, \quad (3b)$$

where $\mathbf{n}_{\text{LED}}$ and $\mathbf{n}_{\text{PD}}$ are the normal vectors at the LED and the receiver planes, respectively, and the symbols $\cdot$ and $\|\cdot\|$ denote the inner product and the Euclidean norm operators,

respectively. Furthermore, Ψ_c denotes the field-of-view (FoV) of the receiver; $\mathcal{G}_f$ is the gain of the optical filter; $\mathcal{G}_c$ is the gain of the optical concentrator given by

$$\mathcal{G}_c = \begin{cases} \dfrac{\varsigma^2}{\sin^2 \Psi_c}, & 0 \leq \psi \leq \Psi_c \\ 0, & \text{otherwise} \end{cases}, \quad (4)$$

where ς stands for the refractive index; m is the Lambertian order which is given by

$$m = -\frac{1}{\log_2(\cos \Phi_{1/2})}, \quad (5)$$

where $\Phi_{1/2}$ is the LED half-intensity angle.

B. Channel gain of reflected paths via IRS

Optical IRSs can be realised by means of metasurfaces or mirror arrays as discussed in [12]. Different to radio frequency (RF) systems, where IRSs can control the phase of the reflected signal, the focus in optical IRSs is to steer the light. Phase control is not directly applicable to VLC systems due to intensity modulation/ direct detection which deals only with the real part of the signal. In this paper, we assume that the IRS is a mirror array consisting of multiple adjacent REs, each of which can be controlled to guide the impinging light towards a desired direction. Since light can be steered to specific point coordinates, each RE can only serve one user at a time, as seen in Fig. 2. The specular reflection path can be considered as an alternative path emitted from the AP to the user. According to Snell's law of reflection, the orientation of each RE needs to be configured such that it reflects the impinging light towards a specific user. Based on that, each IRS RE can serve a single PD at a certain time slot, and the interference from specular reflection paths is negligible.

Each reflected path through the IRS is composed of two components: LED-to-RE path and RE-to-PD path. An approximate expression for the cascaded channel gain under the point source assumption was derived in [12]. Based on this, the cascaded channel gain through the n-th RE is given by

$$h_{k,n,\text{LED}}^{\text{Ref}} = \mathcal{V}_{k,n,\text{LED}}^{\text{Ref}} \cos^m(\phi_{n,\text{LED}}) \cos(\psi_{k,n}), \quad (6)$$

for $0 \leq \psi_{k,n} \leq \Psi_c$ and 0 otherwise, where

$$\mathcal{V}_{k,n,\text{LED}}^{\text{Ref}} = \frac{A(m+1)}{2\pi(d_{n,\text{LED}} + d_{k,n})^2} \mathcal{G}_f \mathcal{G}_c. \quad (7)$$

we assume the REs have unity reflectivity for simplicity. Also, $d_{n,\text{LED}}$ and $d_{k,n}$ denote the Euclidean distance from the LED to the n-th RE and the n-th RE to the k-th user, respectively; $\phi_{n,\text{LED}}$ and $\psi_{k,n}$ are the angle of irradiance and incidence with respect to the axis normal to the receiver plane, calculated as

$$\cos(\phi_{n,\text{LED}}) = \frac{\mathbf{d}_{n,\text{LED}} \cdot \mathbf{n}_{\text{LED}}}{\|\mathbf{d}_{n,\text{LED}}\|}, \quad (8a)$$

$$\cos(\psi_{k,n}) = \frac{\mathbf{d}_{k,n} \cdot \mathbf{n}_{\text{PD}}}{\|\mathbf{d}_{k,n}\|}, \quad (8b)$$

we define the non-line-of-sight (NLoS) channel gain vector $\tilde{\mathbf{h}}_k = [h_{k,1,\text{LED}}^{\text{Ref}}, h_{k,2,\text{LED}}^{\text{Ref}}, \dots, h_{k,n,\text{LED}}^{\text{Ref}}]^T$. Moreover, since each RE can serve one user at a time, we define a binary

IRS allocation vector $\mathbf{g}_k = [g_{k,1}, g_{k,2}, \ldots, g_{k,N}]^T$ such that $g_{k,n} = 1$ of the nth RE is serving the k-th user, and $g_{k,n} = 0$ otherwise.

C. NOMA and the associated information leakage risk

According to the principle of NOMA, the AP allocates a higher power level to the user with lower channel gain and vice versa. The two signals are then superimposed in the power domain and transmitted in a single time/frequency resource block. On the receiver side, the user allocated higher power value can directly decode its intended signal while regarding the interference from the other user's signal as noise. However, the user allocated low power level cannot directly decode its signal and needs to resort to SIC. In SIC, the user decodes and subtracts the information sequence intended for the other user to reach its intended information. The process of SIC necessities that one user decodes the other user's signal, which involves a security threat if that user was malicious. For this reason, we assume that each user is associated with a trust score, which can be obtained based on previous activity or through authentication measures. The user with a lower trust score is treated as a malicious user. In order to reduce the eavesdropping probability, the AP needs to allocate a higher power level to the untrusted user (so that it cannot perform SIC and extract the confidential message). Implementing this power allocation strategy might be challenging in conventional NOMA-based VLC systems that rely merely on the LoS channel paths. This is because the allocated power levels usually depend on the associated channel gain, i.e., higher power is allocated to users with unfavourable channel conditions and vice versa. This challenge can be overcome in IRS-assisted VLC. By configuring the allocation of the IRS REs between the two users to create better conditions for enhanced PLS.

III. JOINT IRS CONFIGURATION AND POWER ALLOCATION FOR ENHANCED PLS

This section proposes a novel PLS approach, formulates a joint IRS configuration and power allocation problem to reduce the risk of eavesdropping, and proposes a solution based on an iterative optimisation algorithm.

A. The proposed strategy

Our goal is to secure the signal of a trusted user, U_t, against a potentially untrusted user, U_u. Since both NOMA users are network users, we need to satisfy the minimum rate constraints for both of them. This means that U_u's minimum rate requirment should be satisfied while, at the same time, minimising its ability to decode the signal of U_t. In the proposed strategy, the power allocation is not performed based on the users' channel gain values but rather based on the trust score, i.e., U_u is always in the first decoding order (always allocated higher power). In this way, U_u decodes its signal directly while U_t performs SIC to subtract the other users's signal and then decode its own signal. According to the concept of NOMA, the transmit signal is:

$$x = P_t s_t + P_u s_u, \tag{9}$$

where s_t and s_u donate the information signal intended to U_t and U_u, respectively; $P_u > P_t$; $P_u + P_t \leq P_{\text{LED}}$. The received signals can be expressed as

$$y_t = \rho \left(h_t^{\text{LoS}} + \tilde{\mathbf{h}}_t^T \mathbf{g}_t \right) (P_u s_u + P_t s_t) + z_t, \tag{10a}$$

$$y_u = \rho \left(h_u^{\text{LoS}} + \tilde{\mathbf{h}}_u^T \mathbf{g}_u \right) (P_u s_u + P_t s_t) + z_u, \tag{10b}$$

where ρ is the PD responsivity; z_t and z_u denote the receiver noise modeled as additive white Gaussian noise (AWGN) with variances σ_t and σ_u. Assuming that the trusted user performs successful SIC, the corresponding signal-to-interference-plus-noise-ratio (SINR) can be written as

$$\gamma_t = \frac{\rho^2 P_t^2 \left(h_t^{\text{LoS}} + \tilde{\mathbf{h}}_t^T \mathbf{g}_t \right)^2}{\sigma_t^2} \tag{11a}$$

$$\gamma_u = \frac{\rho^2 P_u^2 \left(h_u^{\text{LoS}} + \tilde{\mathbf{h}}_u^T \mathbf{g}_u \right)^2}{P_t^2 \left(h_u^{\text{LoS}} + \tilde{\mathbf{h}}_u^T \mathbf{g}_u \right)^2 + \sigma_u^2}. \tag{11b}$$

The classic Shannon capacity formula does not accurately capture the data rates in VLC systems, due to the distinct features of the optical channel as well as the illumination constraints. Alternatively, we utilise the tight lower bound in [13] to calculate the achievable data rates at the users as follows

$$R_t = \frac{1}{2} W \log_2 \left(1 + \frac{e}{2\pi} \frac{\rho^2 P_t^2 \left(h_t^{\text{LoS}} + \tilde{\mathbf{h}}_t^T \mathbf{g}_t \right)^2}{\sigma_t^2} \right) \tag{12a}$$

$$R_u = \frac{1}{2} W \log_2 \left(1 + \frac{e}{2\pi} \frac{\rho^2 P_u^2 \left(h_u^{\text{LoS}} + \tilde{\mathbf{h}}_u^T \mathbf{g}_u \right)^2}{P_t^2 \left(h_u^{\text{LoS}} + \tilde{\mathbf{h}}_u^T \mathbf{g}_u \right)^2 + \sigma_u^2} \right) \tag{12b}$$

where W denotes the modulation bandwidth.

B. Problem formulation

Our objective is to maximise the secrecy capacity of U_t, which can be defined by the tight lower bound in [14] as

$$C_t = \frac{1}{2} W \log_2 \left(\frac{\sigma_u^2}{2\pi\sigma_t^2} \left(\frac{e\rho P_t^2 \left(h_t^{\text{LoS}} + \tilde{\mathbf{h}}_t^T \mathbf{g}_t \right)^2 + 2\pi\sigma_t^2}{\rho P_u^2 \left(h_u^{\text{LoS}} + \tilde{\mathbf{h}}_u^T \mathbf{g}_u \right)^2 + \sigma_u^2} \right) \right). \tag{13}$$

It is noted that, since U_u is an eligible network user, the optimisation approach needs to ensure that the minimum rate requirement of U_u is satisfied. This implies that the resources allocated to U_u (allocated power and REs) facilitate that it can decode its own data signal, s_u, under the presence of interference from U_t's signal, without being able to extract s_t. The optimisation problem is formulated as

$$(\mathcal{P}): \max_{\mathbf{G},\mathbf{P}} C_t, \tag{14a}$$

subject to

$$P_t + P_u \leq P_{\text{LED}}, \tag{14b}$$

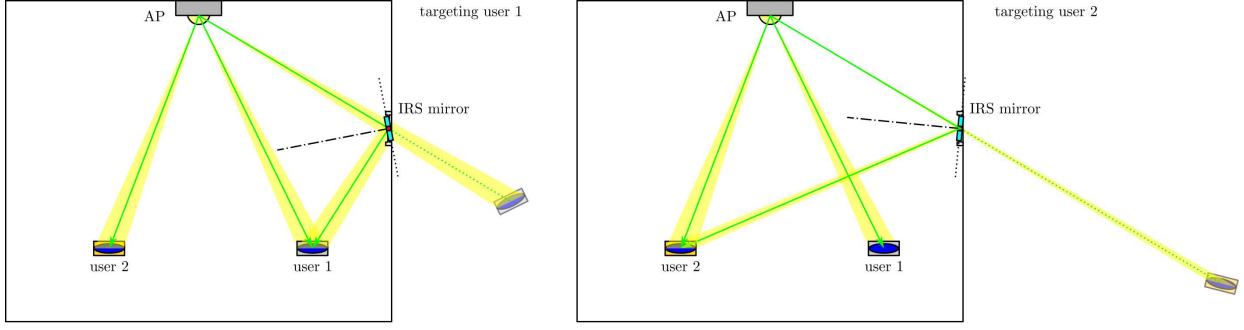$$R_k \geq R_k^{\min}, \forall k \in \{t, u\} \tag{14c}$$

Fig. 2: IRS configuration: each RE can serve one user at a time by steering the reflected light in a certain direction.

$$g_{n,k} \in \{0,1\}, \forall n = 1, 2, \ldots, N, \ k \in \{t, u\} \tag{14d}$$

$$\sum_{k \in t, u} g_{n,k} \in \{0,1\}, \forall n = 1, 2, \ldots, N. \tag{14e}$$

Here, $\mathbf{P} = [P_t, P_u]$ is the NOMA power allocation vector, and $\mathbf{G} = [\mathbf{g_t}, \mathbf{g_u}]$ is the IRS allocation matrix. Constraint (14b) is related to the total transmit power limitation, constraint (14c) ensures that the minimum rate requirements are satisfied, and constraints (14d) and (14e) ensure that each IRS RE can be allocated to a maximum of one user at a time. The optimisation problem (14a) constitutes non-deterministic polynomial (NP)-hard problem. Next, we propose an iterative optimisation algorithm to reach a near-optimal solution.

C. Alternating optimisation algorithm

In order to solve (14a), we split the optimisation problem into two sub-problems, namely $\mathcal{P}_1$ and $\mathcal{P}_2$ that are concerned with optimising a single variable, i.e., $\mathbf{G}$ and $\mathbf{P}$, respectively, while the other variable is fixed. The first sub-problem is the IRS REs allocation optimisation under fixed NOMA power allocation vector $\mathbf{P}$, which can be expressed as

$$(\mathcal{P}_1): \ \max_{\mathbf{G}} C_t(\mathbf{G}), \tag{15a}$$

subject to

$$R_k \geq R_k^{\min}, \forall k \in \{t, u\} \tag{15b}$$

$$0 \leq g_{n,k} \leq 1 \quad \forall n = 1, 2, \ldots, N, \ k \in \{t, u\} \tag{15c}$$

$$\sum_{k \in t, u} g_{n,k} \in \{0,1\}, \forall n = 1, 2, \ldots, N. \tag{15d}$$

Note that by relaxing the constraint in (14d) to (15c), we obtain a linear programming problem that can be solved by means of the CVX toolbox [32]. We then employ a greedy policy to recover the discreteness of $\mathbf{G}$ as shown in steps 3-7 of Algorithm 1.

D. Adaptive-restart GA

Once the IRS allocation matrix $\mathbf{G}$ is obtained, we solve the NOMA power allocation problem for fixed $\mathbf{G}$ as follows

$$(\mathcal{P}_2): \ \max_{\mathbf{P}} C_t, \tag{16a}$$

subject to

$$R_k \geq R_k^{\min}, \forall k \in \{t, u\} \tag{16b}$$

Algorithm 1: Alternating optimisation algorithm

Input: h_t^{LoS}, h_u^{LoS}, $\tilde{\mathbf{h}}_t, \tilde{\mathbf{h}}_u$, $R_t^{\min}$, $R_u^{\min}$, δ_1.
Output: $\mathbf{G}$ and $\mathbf{P}$
1 **Init:** $i \leftarrow 0$, initialise $\mathbf{G}^{(0)}$ and $\mathbf{P}^{(0)}$ as random feasible solutions to $\mathcal{P}$.
2 **repeat:** Given $\mathbf{P}^{(i)}$ solve $\mathcal{P}_1$ to obtain IRS allocation matrix $\mathbf{G}^{(i)}$;
3 **for** *n=0:N* **do**
4 $\quad$ $k_\dagger \leftarrow \min_k g_{n,k_\dagger}$;
5 $\quad$ $g_{n,k_\dagger} \leftarrow 1$ and $g_{n,k \neq k_\dagger} \leftarrow 0$;
6 $\quad$ $n \leftarrow n + 1$;
7 **end**
8 Given $\mathbf{G}^{(i+1)}$ solve $\mathcal{P}_2$ by GA to obtain power allocation vector $\mathbf{P}^{(i+1)}$;
9 **until:** $|C_t(\mathbf{G}^{i+1}, \mathbf{P}^{i+1}) - C_t(\mathbf{G}^{i+1}, \mathbf{P}^{i+1})| < \delta_1$

$$P_t + P_u \leq P_{\mathrm{LED}}. \tag{16c}$$

In order to obtain a solution for $\mathcal{P}_2$, we utilise adaptive-restart GA presented in Algorithm 2, which is known to be an effective heuristic technique for obtaining computationally-efficient near-optimal solutions. Its working principle mimics the idea of natural evolution based on the idea of the "survival of the fittest". As shown in Algorithm 2, we start with an initial population of chromosomes, each representing a possible solution for $\mathbf{P}$. In each iteration of the algorithm, a mutation operation is applied to the current population in order to generate slightly modified chromosomes for the following generation, followed by a crossover operation that generates new instances of $\mathbf{P}$ within the search space of candidate solutions. The fitness of each candidate solution is evaluated in each iteration based on (16a) and the associated constraints. Based on that, a selection process is performed to carry the fittest solutions to the next iteration and discard the bad solutions. To enhance the global search capability of the GA and reduce the probability of converging to a local optimum, We employ an adaptive-restart mechanism [15]. This is represented by the outer *for* loop in Algorithm 2 which restarts the GA with some "elite" quality chromosomes generated in the previous iteration.

Algorithm 2: Adaptive-restart genetic algorithm

Input: Population size, $\mathcal{S}$, number of generations, N_{Gen}, maximum run time, $t_{\max}$, h_t^{LoS}, h_u^{LoS}, $\hat{\mathbf{h}}_t$, $\hat{\mathbf{h}}_u$, $R_t^{\min}$, $R_u^{\min}$, $\mathbf{G}$.

Output: Global best solution $\mathbf{P}$.

1 **Start:**
2 Generate initial population of $\mathcal{S}$ chromosomes $\mathcal{Y}_0$;
3 Set time counter $t = 0$;
4 **while** $t < t_{\max}$ **do**
5   **for** $i = 1 : N_{\text{Gen}}$ **do**
6   **for** $j = 1 : N_{\text{Gen}}$ **do**
7   Select a pair of chromosomes from $\mathcal{Y}_{j-1}$;
8   Apply crossover operation on selected pair with crossover probability $\mathcal{P}_c$;
9   Apply mutation operation on the offspring with mutation probability $\mathcal{P}_m$;
10   Check constraints (16b)-(16c) and repair;
11   Evaluate the fitness of each chromosome in $\mathcal{Y}_j$ using (16a); Select elite chromosomes;
12   **end**
13   Update $\mathcal{Y}_{\text{best}}$;
14   Restart with an adaptive initial population $\tilde{\mathcal{Y}}(i + 1)$ containing the elite chromosomes;
15   **end**
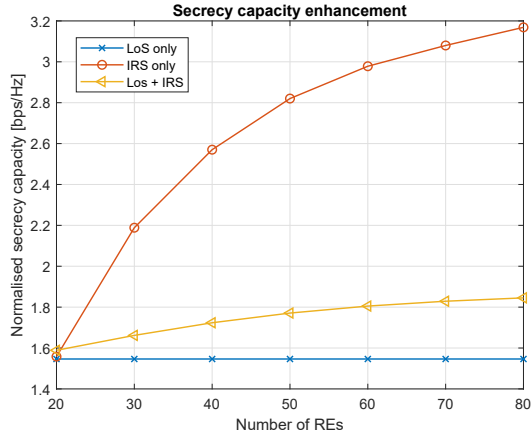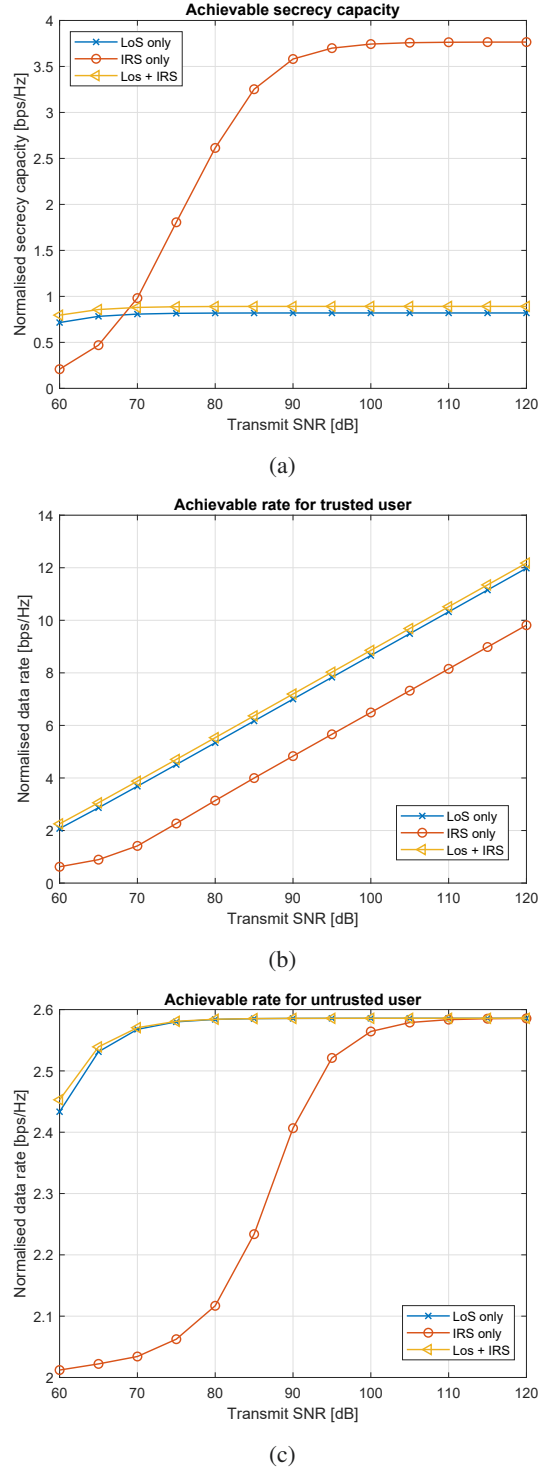16 **end**

(a)

(b)

(c)

Fig. 4: The achievable performance in terms of (a) achievable secrecy capacity, (b) achievable rate of U_t, and (c) achievable rate of U_u, for an IRS fixed on one wall with 40 REs.

Fig. 3: The achievable secrecy capacity of U_t vs the number of REs for transmit SNR of 80 dB.

IV. RESULTS AND DISCUSSIONS

In this section, we present the simulation results for two NOMA users located in a $3 \times 3 \times 5$ room. The transmitting LED AP is fixed at the centre of the ceiling and the users' locations are randomly generated across the room for a number of 10^3 iterations in order to capture the average system performance. We assume that an IRS consisting of N REs is fixed on the wall. Moreover, we assume that the AP has prior knowledge of the trust score of both users such that the user with a higher trust score is labeled as a trusted user, U_t, and the user with a lower trust score is labeled as an untrusted user, U_u. Based on the discussion in Section III, U_u is assigned the first SIC decoding order to reduce the risk of information leakage.

Fig. 3 presents the normalised secrecy capacity of U_t under the proposed scheme vs the number of REs. It can be seen that using combined LoS and IRS links can slightly increase the secrecy capacity performance and that the enhancement becomes more pronounced as the number of REs increases.

5

However, the performance enhancement can be considered limited and does not exceed 20%. This is attributed to the fact that the LoS channel gain in VLC remains dominant even for a high number of REs. Fig. 3 also shows the performance enhancement when only IRS links are utilised for communications. We can see that the secrecy capacity can be greatly enhanced with an improvement of up to 105% for 80 REs. This result might look confusing as the users experience much lower channel gain when there is no LoS between the user and the AP, Nonetheless, the performance enhancement here stems from the fact that the secrecy capacity is reliant on the relative channel gain values of the trusted users and the eavesdropper. In the absence of direct LoS links, the IRS gives a great flexibility and a high degree of freedom to manipulate the users' channel conditions so as to maximise the achievable secrecy capacity.

In order to get more insights on the rate performance of the NOMA users under the proposed scheme, we present the secrecy capacity of the trusted user as well as the individual achievable data rates, for a fixed number of REs of $N = 40$, across a transmit SNR range of $60 - 120$ dB. We can observe from Fig. 4 that utilising 'IRS only' links provides prominent secrecy capacity enhancement for medium to high SNR values. It is clear that, under low SNR, depending on the IRS will not be sufficient. The 'IRS only' strategy results in slight rate degradation for U_t and a severe rate degradation for U_u, However, U_u rate is kept higher that the minimum rate defined by the optimisation constraint in (15c). Hence, the proposed scheme maximises the secrecy capacity while satisfying the rate constraints at both NOMA users. We note that the LoS in VLC cannot be simply switched off so that the user only receives the reflected paths, however, we believe that the proposed results open the door for investigating novel VLC setups in which the transmission links are fully controlled by means of IRSs. For example, by using LEDs with narrow FoV that can be directed towards and IRS so that the users do not perceive the LoS and depend on the IRS reflections.

V. Conclusion

This paper proposed a PLS mechanism for mitigating the information leakage risk in NOMA VLC systems. The idea is based on utilising IRSs to control the channel gains at the users, and hence the ability of an untrusted user to decode a confidential signal. We have demonstrated that jointly optimising the IRS configuration and NOMA power allocation can enhance the secrecy capacity and reduce the possibility of eavesdropping by a potentially malicious network user. Our results revealed that utilising IRS paths only without LoS gives the highest degree of freedom and, thus, the highest possible secrecy capacity, albeit with a decrease in the achievable data rates. Although depending on IRS reflected paths without a LoS link might not be ideal from an energy efficiency perspective, we believe that the presented results offer valuable insights on how IRSs can be integrated into NOMA-based VLC systems, particularly under LoS blockage conditions.

References

[1] H. Haas, E. Sarbazi, H. Marshoud, and J. Fakidis, "Chapter 11 - visible-light communications and light fidelity," *Optical Fiber Telecomm. VII*, pp. 443–493, 2020.

[2] H. Haas *et al.*, "Introduction to indoor networking concepts and challenges in LiFi," *IEEE/OSA J. Opt. Commun. Netw.*, vol. 12, no. 2, pp. A190–A203, 2020.

[3] J. Lian and M. Brandt-Pearce, "Multiuser visible light communication systems using OFDMA," *J. Lightw. Technol.*, vol. 38, no. 21, pp. 6015–6023, 2020.

[4] H. Abumarshoud, H. Alshaer, and H. Haas, "Dynamic multiple access configuration in intelligent LiFi attocellular access points," *IEEE Access*, vol. 7, pp. 62 126–62 141, 2019.

[5] H. Abumarshoud *et al.*, "LiFi through reconfigurable intelligent surfaces: A new frontier for 6G?" *IEEE Veh. Technol. Mag.*, pp. 2–11, 2021.

[6] B. Cao *et al.*, "Reflecting the light: Energy efficient visible light communication with reconfigurable intelligent surface," *in Proc. IEEE 92nd Vehicular Technology Conference (VTC2020-Fall)*, pp. 1–5, Feb. 2021.

[7] S. Sun, F. Yang, and J. Song, "Sum rate maximization for intelligent reflecting surface-aided visible light communications," *IEEE Commun. Lett.*, pp. 1–1, 2021.

[8] H. Abumarshoud, B. Selim, M. Tatipamula, and H. Haas, "Intelligent reflecting surfaces for enhanced NOMA-based visible light communications," in *ICC 2022 - IEEE International Conference on Communications*, 2022, pp. 571–576.

[9] M. A. Arfaoui, M. D. Soltani, I. Tavakkolnia, A. Ghrayeb, M. Safari, C. M. Assi, and H. Haas, "Physical layer security for visible light communication systems: A survey," *IEEE Commun. Surveys Tuts.*, vol. 22, no. 3, pp. 1887–1908, 2020.

[10] H. Abumarshoud, C. Chen, M. S. Islim, and H. Haas, "Optical wireless communications for cyber-secure ubiquitous wireless networks," *Proceedings of the Royal Society A: Mathematical, Physical and Engineering Sciences*, vol. 476, no. 2242, Oct. 2020.

[11] H. Abumarshoud, M. D. Soltani, M. Safari, and H. Haas, "Realistic secrecy performance analysis for LiFi systems," *IEEE Access*, vol. 9, pp. 120 675–120 688, 2021.

[12] A. M. Abdelhady *et al.*, "Visible light communications via intelligent reflecting surfaces: Metasurfaces vs mirror arrays," *IEEE Open J. of the Commun. Soc.*, vol. 2, pp. 1–20, Dec. 2021.

[13] J.-B. Wang, Q.-S. Hu, J. Wang, M. Chen, and J.-Y. Wang, "Tight bounds on channel capacity for dimmable visible light communications," *J. Lightw. Technol.*, vol. 31, no. 23, pp. 3771–3779, 2013.

[14] J.-Y. Wang, C. Liu, J.-B. Wang, Y. Wu, M. Lin, and J. Cheng, "Physical-layer security for indoor visible light communications: Secrecy capacity analysis," *IEEE Trans. Commun.*, vol. 66, no. 12, pp. 6423–6436, 2018.

[15] F. Ghannadian, C. Alford, and R. Shonkwiler, "Application of random restart to genetic algorithms," *Information Sciences*, vol. 95, no. 1, pp. 81–102, 1996.